Ozone stratospheric trends from regional Bayesian composite of ground-based partial columns

Louis Miralllie[1, 2, 3], Eliane Maillard Barras[1], Caroline Jonas[4], Corinne Vigouroux[4], Roeland Van Malderen[5], Irina Petropavlovskikh[6, 7], Sophie Godin-Beekmann[8], Thierry Leblanc[9], Wolfgang Steinbrecht[10], Antoine Vadès[11], Rolf Ruefenacht[1], Alexander Haefele[1], Gunter Stober[2, 3], Peter Effertz[6, 7], Julian Gröbner[12], Gerard Ancellet[8], María Cazorla[13], Petra Duff[14], Matthias M. Frey[15], Michael Gill[16], James W. Hannigan[17], Nicholas Jones[18], Rigel Kivi[19], Raphael Köhler[20], Bogumil Kois[21], Debra E. Kollonige[22, 23], Emmanuel Mahieu[24], Glen McConville[7], Johan Mellqvist[25], Gary Morris[7], Isao Murata[26], Tomoo Nagahama[27], Gerald E. Nedoluha[28], Shin-Ya Ogino[29], Richard Querel[30], Ryan M. Stauffer[22], Wolfgang Stremme[31], Kimberly Strong[14], Ralf Sussmann[32], Anne M. Thompson[22, 33], Yana Virolainen[34]

[1] Federal Office of Meteorology and Climatology, MeteoSwiss, Payerne, Switzerland
[2] Institute of Applied Physics, Microwave, University of Bern, Bern, Switzerland
[3] Oeschger Center for Climate Change Research, Microwave Physics, University of Bern, Bern, Switzerland
[4] Royal Belgian Institute for Space Aeronomy (BIRA-IASB), Uccle, Belgium
[5] Royal Meteorological Institute, Uccle, Belgium
[6] Cooperative Institute for Research in Environmental Sciences, University of Colorado, Boulder, CO, USA
[7] NOAA Global Monitoring Laboratory, Boulder, CO, USA
[8] LATMOS/IPSL, Sorbonne Université, UVSQ, CNRS, Paris, France
[9] Jet Propulsion Laboratory, California Institute of Technology, Wrightwood, California, USA
[10] Deutsche Wetterdienst, Hohenpeißenberg, Germany
[11] Formerly at Federal Office of Meteorology and Climatology, MeteoSwiss, Payerne, Switzerland
[12] Physikalisch-Meteorologisches Observatorium Davos World Radiation Centre, Dorfstrasse 33, 7260 Davos Dorf, Switzerland
[13] Instituto de Investigaciones Atmosféricas, Universidad San Francisco de Quito USFQ, Quito, Ecuador
[14] Department of Physics, University of Toronto, Toronto, ON, Canada
[15] Institute for Meteorology and Climate Research Atmospheric Trace Gases and Remote Sensing (IMKASF), Karlsruhe Institute of Technology (KIT), Karlsruhe, Germany
[16] Met Éireann Valentia Observatory, Cahersiveen, Co. Kerry, Ireland
[17] National Center for Atmospheric Research, Boulder, CO, USA
[18] University of Wollongong, Wollongong NSW, Australia
[19] Space and Earth Observation Centre, Finnish Meteorological Institute, Sodankylä, Finland
[20] Alfred Wegener Institute, Helmholtz Centre for Polar and Marine Research, Potsdam, Germany
[21] Institute of Meteorology and Water Management – National Research Institute (IMGW-PIB), Poland
[22] Earth Sciences Division, NASA Goddard Space Flight Center, Greenbelt, Maryland, USA
[23] ADNET Systems, Inc., Bethesda, Maryland, USA
[24] Department of Astrophysics, Geophysics and Oceanography, UR SPHERES, University of Liège, Liège, Belgium
[25] Space Earth and Environment , Chalmers University of technology, 41296 Göteborg, Sweden
[26] Graduate School of Environmental Studies, Tohoku University, Sendai, Japan
[27] Institute for Space-Earth Environmental Research, Nagoya University, Nagoya, Japan
[28] Naval Research Laboratory, 4555 Overlook Avenue, SW, Washington, D.C. 20375, USA
[29] Japan Agency for Marine-Earth Science and Technology (JAMSTEC), Research Institute for Global Change, Yokosuka, Japan
[30] Earth Sciences New Zealand (ESNZ), Lauder, New Zealand
[31] Instituto de Ciencias de la Atmósfera y Cambio Climático, Universidad Nacional Autonoma de Mexico (UNAM), Mexico City, MEXICO
[32] Karlsruhe Institute of Technology (KIT), IMKIFU, Garmisch-Partenkirchen, Germany

[33] University of Maryland - Baltimore County, Baltimore, Maryland, USA
[34] St.Petersburg State University, St.Petersburg, Russia
Correspondence to: Louis Mirallie (louis.mirallie@meteoswiss.ch)

S1: All the instruments with availability

Type	Name	Latitude	Longitude	Time range	Major gaps / Remarks	
FTIR	Altzomoni	19.12	-98.66	2012-2022		
	Boulder	39.99	-105.26	2010-2024	2018	
	Bremen	53.1	8.85	2004-2024	2016, 2011	
	Eureka	80.05	-86.42	2006-2020	2012, 2013	Polar night gaps
	Harestua	60.2	10.8	1994-2024	2016, 2023	
	Hefei	31.91	117.17	2015-2023		
	Izana	28.3	-16.48	1999-2023		
	Jungfraujoch	46.55	7.98	1994-2024	2021	
	Kiruna	67.84	20.4	1996-2022		Polar night gaps
	Lauder	-45.04	169.68	2001-2024		
	Maido	-21.1	55.4	2013-2024	2020-2021	
	Mauna Loa	19.54	-155.57	1995-2022	2001-2005, 2011	
	Ny-Ålesund	78.92	11.92	1992-2024	2012, 2014	Polar night gaps
	Rikubetsu	43.46	143.77	1995-2024	2011-2014	
	Saint-Denis	-20.9	55.5	2004-2011	2004-2007, 2008-2009	
	St Petersburg	59.9	29.8	2009-2024	2020	
	Thule	76.53	-68.74	2000-2024		Polar night gaps
	Toronto	43.66	-79.40	2002-2024		
	Tsukuba	36.05	140.12	2001-2024	2001-2014	
	Wollongong	-34.41	150.88	1996-2024		
	Zugspitze	47.42	10.98	2000-2024		
O3S	Alert	82.49	-62.34	1987-2024		no uncertainties after 2015
	Ascension	-7.58	-14.24	1998-2022	2010-2016, 2019	
	Boulder	40	-105.25	1967-2024		

	Edmonton	53.54	-114.1	1970-2021		no uncertainties after 2015
	Eureka	79.98	-85.94	1992-2021		no uncertainties after 2015
	Hanoi	21.01	105.8	2004-2021		sparse
	Hilo	19.43	-155.04	1982-2024		
	Hohenpeissenberg	47.8	11.01	1966-2024		
	Kelowna	49.93	-119.4	2003-2017		
	Kuala Lumpur	2.73	101.27	1998-2022	2010-2012	
	l'Aquila	42.38	13.31	1994-2024	2000-2003	
	Lauder	-45.04	169.68	1986-2024		
	Legionowo	52.4	20.97	1993-2024		
	Lerwick	60.13	-1.18	1992-2024	2002	
	Madrid	40.47	-3.58	1994-2024	2002-2005	
	Nairobi	-1.27	36.8	1998-2024	2020	
	Natal	-5.42	-35.38	1998-2023	2011-2013	
	Ny Alesund	78.92	11.93	1992-2024		
	OHP	43.94	5.71	1991-2024		Large Unc
	Payerne	46.81	6.94	2002-2024		
	Resolute	74.7	-94.96	1966-2024		
	San Cristobal	-0.92	-89.62	1998-2023	2008-2014, 2016-2021	
	Scoresbysund	70.48	-21.97	1989-2024		
	Sodankyla	67.37	26.65	1994-2024		
	Trinidad Head	40.8	-124.16	1997-2024		
	Uccle	50.8	4.35	1969-2024		
	Valentia	51.94	-10.25	1994-2024	2004-2006	
	Watukosek	-7.5	112.6	1998-2022	2013-2021	
	Yarmouth	43.87	-66.11	2003-2021		no uncertainties after 2015

Type	Name	Latitude	Longitude	Time range	Gaps	Remarks

UMKEHR	U256 (Lauder)	-45.04	169.68	2000-2024	2002	
	U31 (Mauna Loa)	19.54	-155.58	2000-2024	2023	
	U35 (Arosa/Davos)	46.78	9.68	1979-2024		
	U40 (OHP)	43.94	5.71	2000-2024		
	U67 (Boulder)	39.99	-105.26	2000-2024		
MWR	Bern	46.95	7.45	1996-2024		
	Payerne	46.81	6.94	2000-2024		
	Lauder	-45.04	169.68	2000-2016	2004, 2014	
	Mauna Loa	19.54	-155.58	1996-2022		
Lidar	OHP	43.94	5.71	1985-2025		
	Hohenpeissenberg	47.8	11.02	1997-2024		
	Mauna Loa	19.54	-155.58	1997-2023		
	Lauder	-45.04	169.68	1997-2024	2014, 2022-2023	
	TMF	34.38	-117.68	1997-2024	1999-2000, 2014-2016	

Table S1: Instruments with metadata. In green, we represent the dataset with a complete time range (2000-2024), no gaps and no missing uncertainties.

S2: Regional Groups

Groups	O3Sondes	FTIR	Umkehr	Lidar	MWR
Europe		Zugspitze, Bremen, Jungfraujoch, Harestua, St Petersbourg	Arosa/Davos, OHP	Hohenpeissenberg, OHP	Bern, Payerne
Scandinavia		Kiruna, Harestua, St Petersburg			
North Canada+ Svalbard		Eureka, Thule, Ny Alesund			

Oceania		Lauder, Wollongong	Lauder	Lauder	Lauder
Mid Latitudes		Zugspitze, Bremen, Jungfraujoch, Harestua, St Petersburg, Izana, Toronto, Boulder, Rikubetsu, Tsukuba, Hefei, Mauna Loa, Altzomoni	Arosa/Davos, OHP, Boulder, Mauna Loa	Hohenpeissenberg, OHP, Table Mountain facility, Mauna Loa	Bern, Payerne, Mauna Loa

Table S2: Group composition in Upper stratosphere (UpS and aUpS).

Groups	O3Sondes	FTIR	Umkehr	Lidar	MWR
Central Europe	Payerne, Uccle, Legionowo, Hohenpeissenberg	Zugspitze, Bremen, Jungfraujoch	Arosa/Davos	Hohenpeissenberg	Bern, Payerne
Scandinavia	Sodankyla, Lerwick	Kiruna, Harestua, St Petersburg, Lerwick			
South Europe	OHP, L'Aquila, Madrid		OHP	OHP	
North Europe	Valentia, Uccle, Legionowo	Bremen, Harestua			
Svalbard+ Greenland	Ny Alesund, Scoresbysund	Ny Alesund			
North Canada	Eureka, Resolute, Alert	Eureka, Thule			
South Canada	Kelowna, Edmonton				
East Coast	Yarmouth	Toronto			
West US	Boulder, Trinidad head	Boulder	Boulder	TMF	
Japan/China		Rikubetsu, Tsukuba, Hefei			
Tropic cancer	Hilo, Hanoi	Mauna Loa, Altzomoni	Mauna Loa	Mauna Loa	Mauna

					Loa
Equator	Kuala Lumpur, Nairobi, Natal, San Cristobal				
South atlantic+ Watukosek	Ascension, Natal, Watukosek				
Lauder	Lauder	Lauder	Lauder	Lauder	Lauder

Table S3: Group composition in Middle stratosphere (MS and aMS).

Groups	O3Sondes	FTIR	Umkehr	Lidar	MWR
Central Europe + OHP	Payerne, Uccle, Legionowo, Hohenpeissenberg, OHP	Zugspitze, Bremen, Jungfraujoch	Arosa/Davos, OHP	Hohenpeissenberg, OHP	
Scandinavia	Sodankyla	Kiruna, Harestua, St Petersburg			
South Europe	OHP, L'Aquila, Madrid		OHP	OHP	
North Sea + Lerwick	Valentia, Uccle, Lerwick				
Svalbard+ Greenland	Ny Alesund, Scoresbysund	Ny Alesund			
North Canada	Eureka, Resolute, Alert, Ny Alesund	Eureka, Thule, Ny Alesund			
South Canada	Kelowna, Edmonton				
East Coast	Yarmouth	Toronto			
West US	Boulder, Trinidad head	Boulder	Boulder	TMF	
Hawaii	Hilo	Mauna Loa	Mauna Loa	Mauna Loa	

Equator & Acsension	Kuala Lumpur, Nairobi, Natal, San Cristobal, Ascension				
Lauder	Lauder	Lauder	Lauder	Lauder	

Table S4: Group composition in Lower stratosphere (LS and UTLS).

Groups	O3Sondes	FTIR	Umkehr	Lidar	MWR
Central Europe	Payerne, Uccle, Hohenpeissenberg	Zugspitze, Bremen, Jungfraujoch			
Scandinavia	Sodankyla	Kiruna, Harestua, St Petersburg			
North Canada	Eureka, Resolute, Alert	Eureka, Thule			
South Canada	Kelowna, Edmonton				
Hawaii	Hilo	Mauna Loa			
Lauder	Lauder	Lauder			

Table S5: Group composition in Troposphere (TROPO and aTROPO).

S3: Composite time series in Troposphere

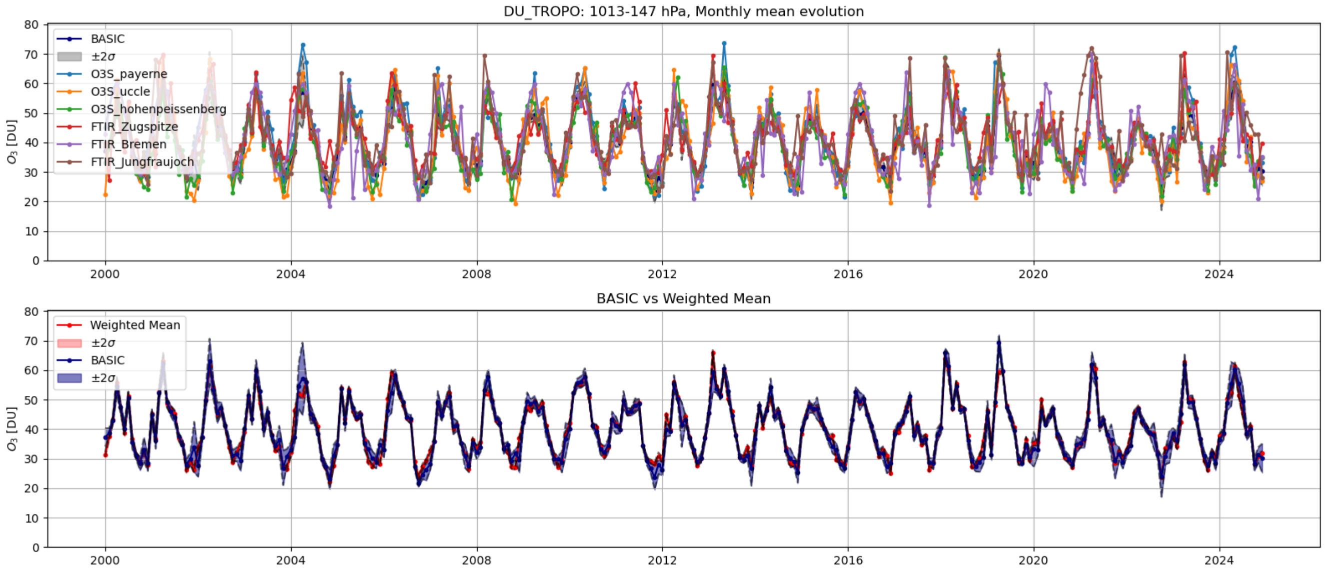

Figure S1: Time series for regional group Central Europe, in TROPO. Top: time series of the group members, plotted with BASIC in blue and its uncertainty in grey. Bottom: comparison between BASIC in blue, with 2 uncertainties in blue, and the Weighted mean in red, with 2 uncertainties in red.

S4: Maps of trends

In the following, we provide maps of trends for the TROPO in oPC and for the layers aUpS, aMS and aTROPO in aPC.

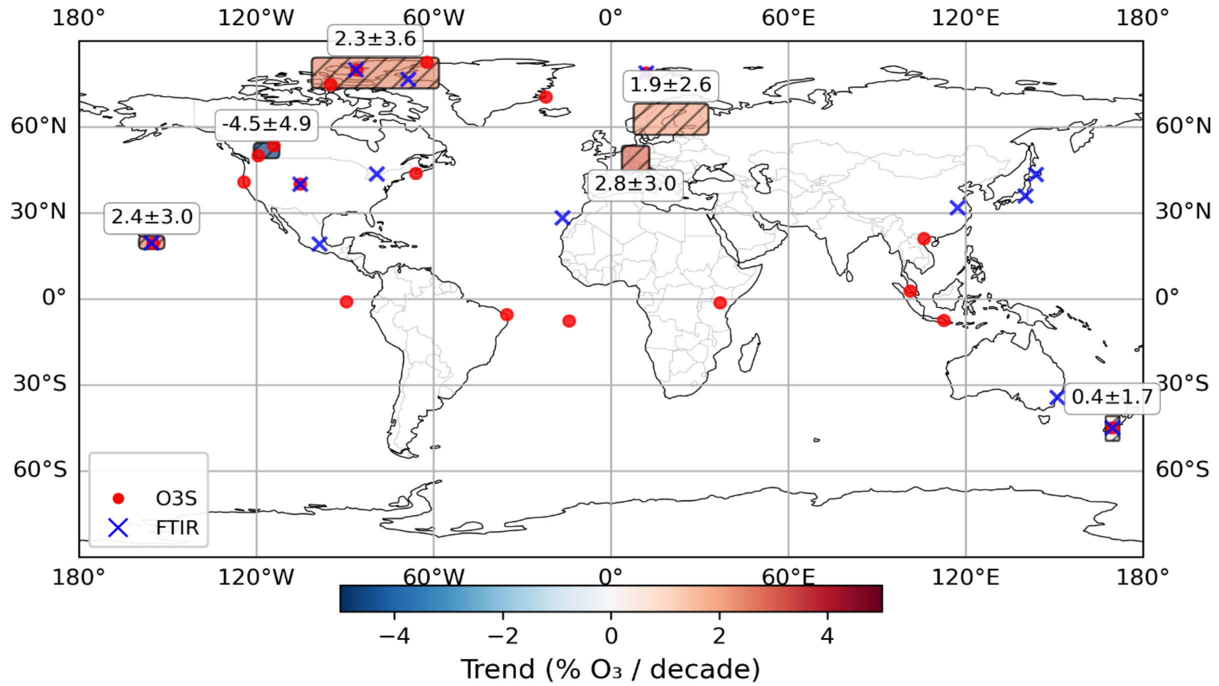

Figure S2: Ozone trends for the regional groups in the troposphere (TROPO). Bold numbers indicate significant trends. The colour scale indicates the trend magnitude: red for positive and blue for negative values. Regions are hatched where trends are not significant at the 95% confidence level (2 sigma). The locations of the instruments merged into the composite are indicated by markers, except in Europe for readability.

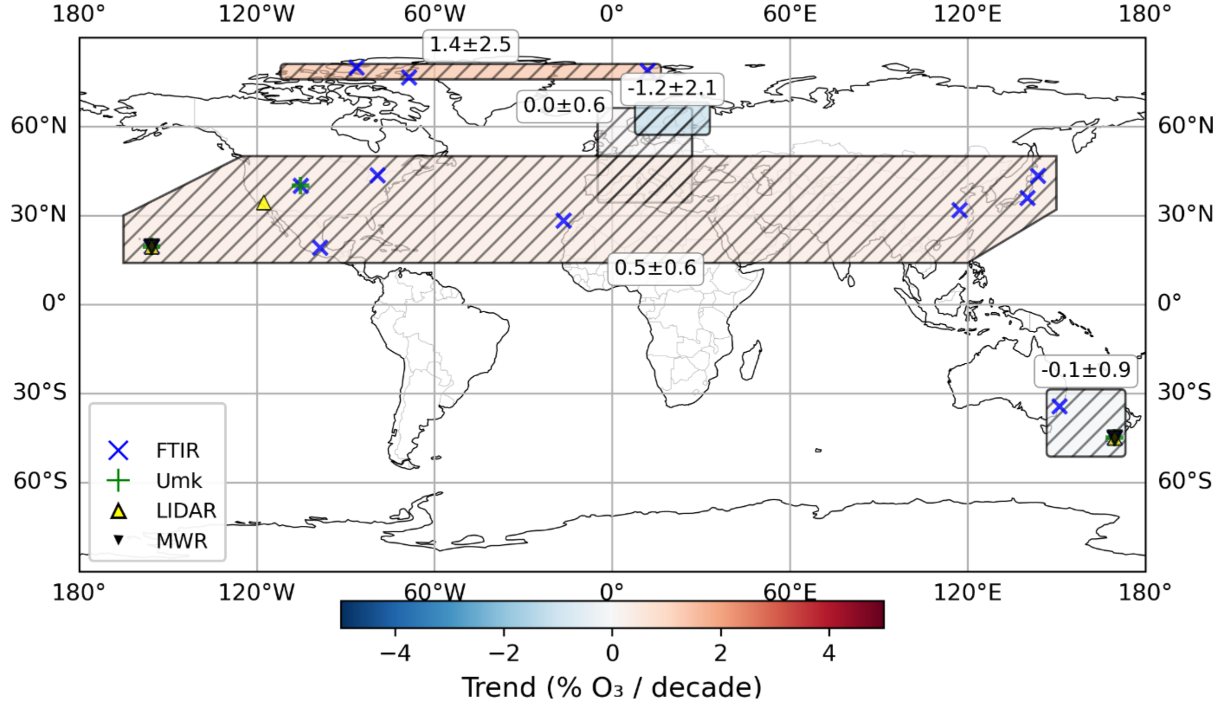

Figure S3: Ozone trends for the regional groups in the alternative upper stratosphere (aUpS). Bold numbers indicate significant trends. The colour scale indicates the trend magnitude: red for positive and blue for negative values. Regions are hatched where trends are not significant at the 95% confidence level (2 sigma). The locations of the instruments merged into the composite are indicated by markers, except in Europe for readability.

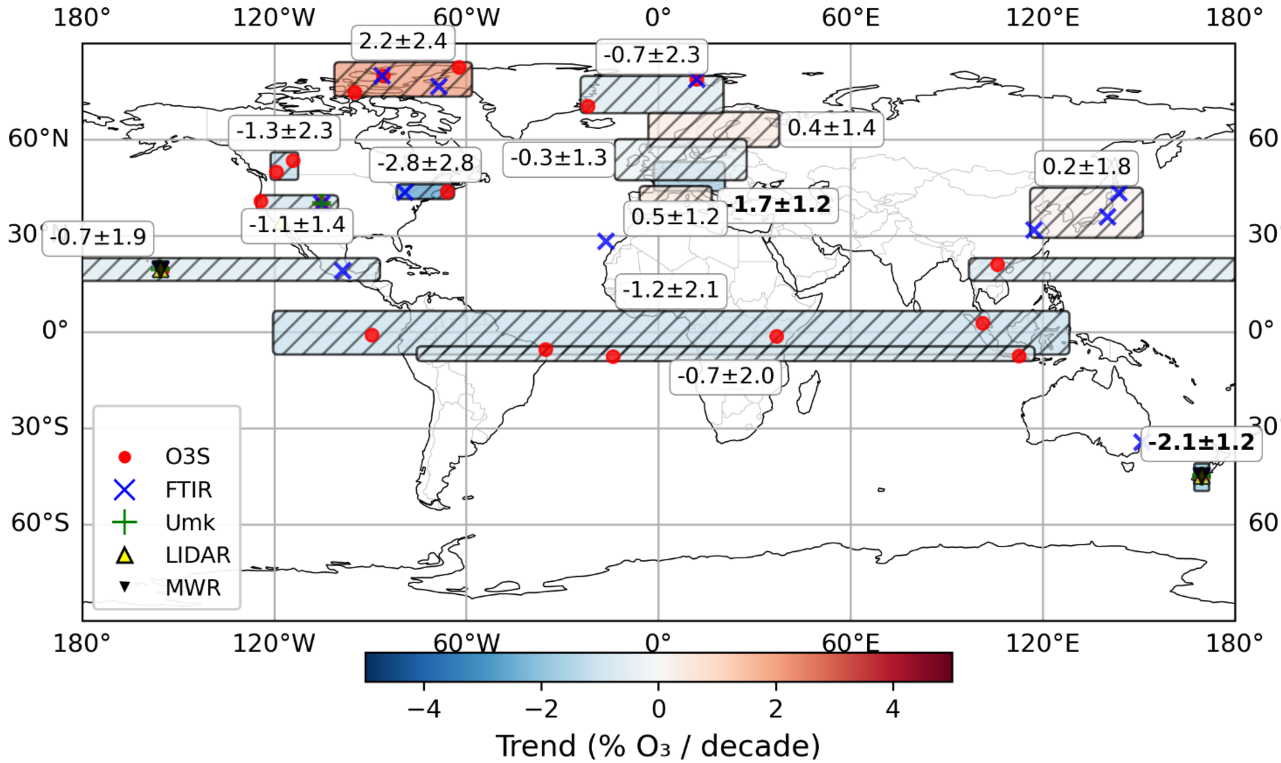

Figure S4: Ozone trends for the regional groups in the alternative middle stratosphere (aMS). Bold numbers indicate significant trends. The colour scale indicates the trend magnitude: red for positive and blue for negative values. Regions are hatched where trends are not significant at the 95% confidence level (2 sigma). The locations of the instruments merged into the composite are indicated by markers, except in Europe for readability.

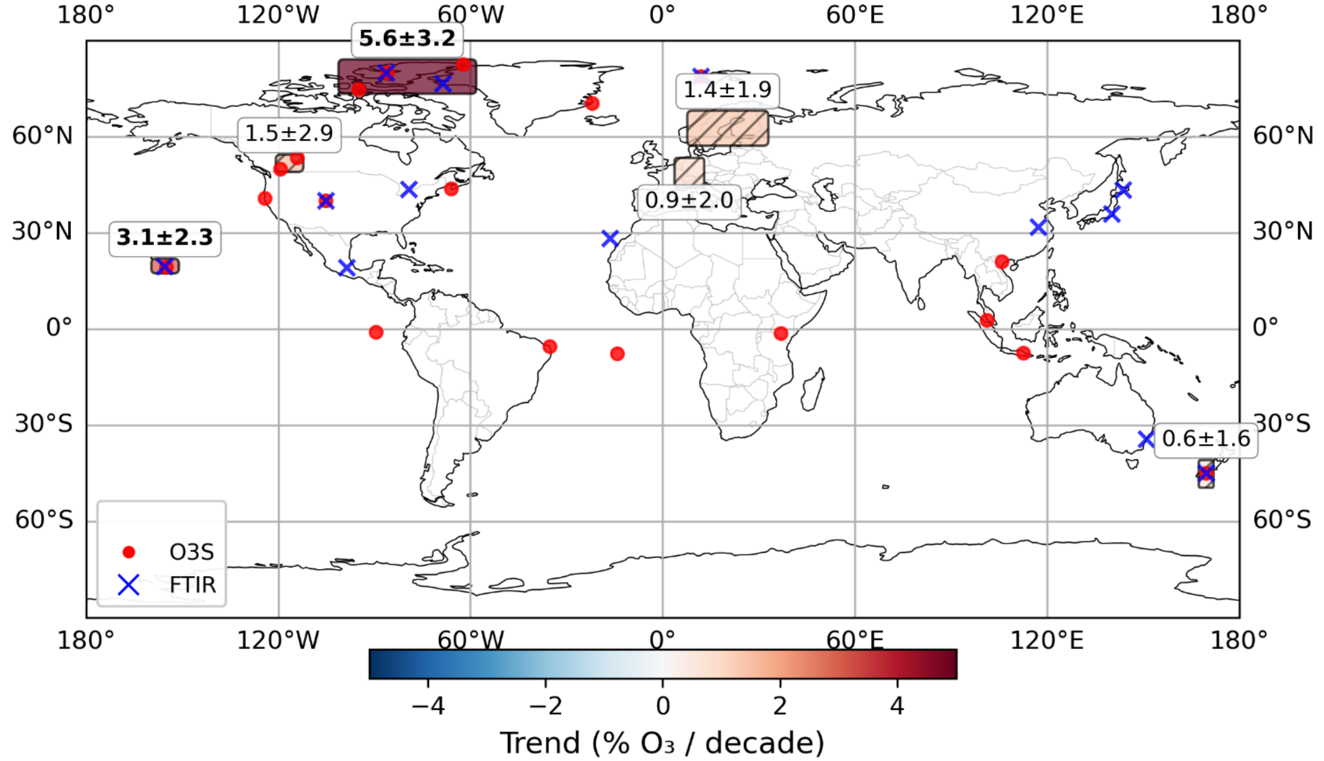

Figure S5: Ozone trends for the regional groups in the alternative troposphere (aTROPO). Bold numbers indicate significant trends. The colour scale indicates the trend magnitude: red for positive and blue for negative values. Regions are hatched where trends are not significant at the 95% confidence level (2 sigma). The locations of the instruments merged into the composite are indicated by markers, except in Europe for readability.

S5: Proxy metadata

Name	Time range	Last accessed	source
QBO	1979-01 2025-10	2025-11-18	https://acdext.gsfc.nasa.gov/Data_services/met/qbo/QBO_EOF_coeff.txt
Solar	1749-01 2025-10	2025-11-18	https://services.swpc.noaa.gov/json/solar-cycle/observed-solar-cycle-indices.json

ENSO	1979-01 2025-07	April 2026	https://psl.noaa.gov/enso/mei/
sAOD	1979-01 2024-12	April 2026	https://www.earthdata.nasa.gov/data/catalog/larc-cloud-glossac-2.23
LOTUS MLR	Version 0.8.3	December 2025	https://usask-arg.github.io/lotus-regression/

Table A5: Explanatory variables time range, source and date of last access

S6: Maps of groups

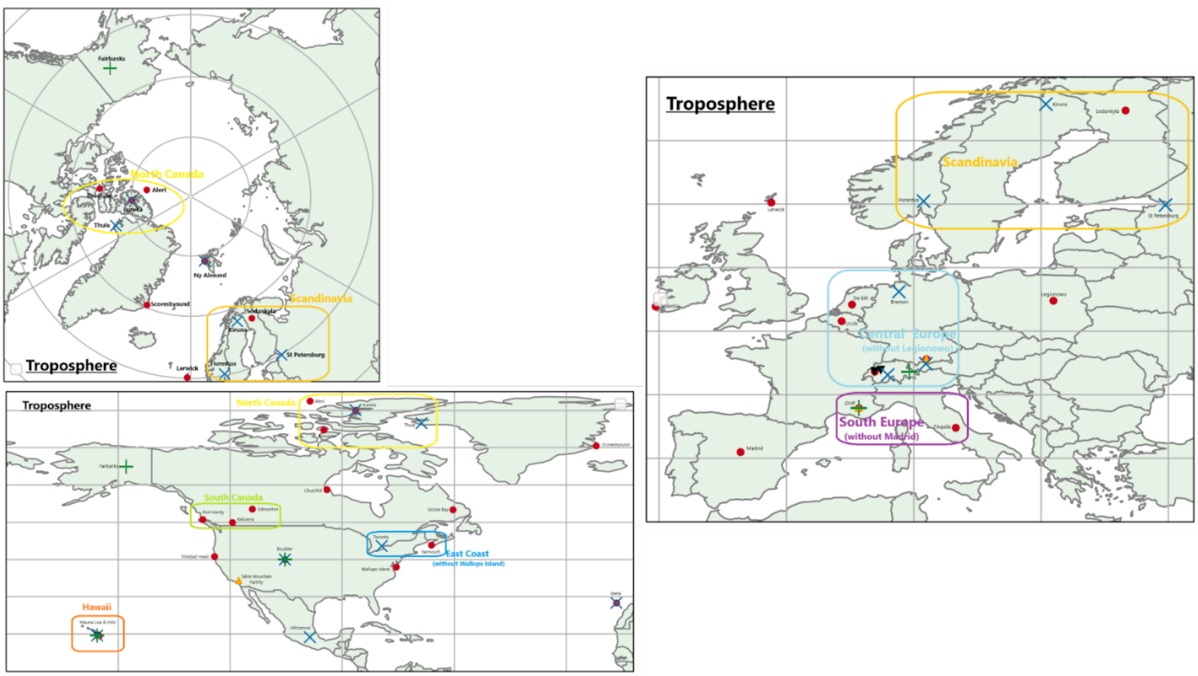

Figure S6: Maps with the groups in TROPO and aTROPO

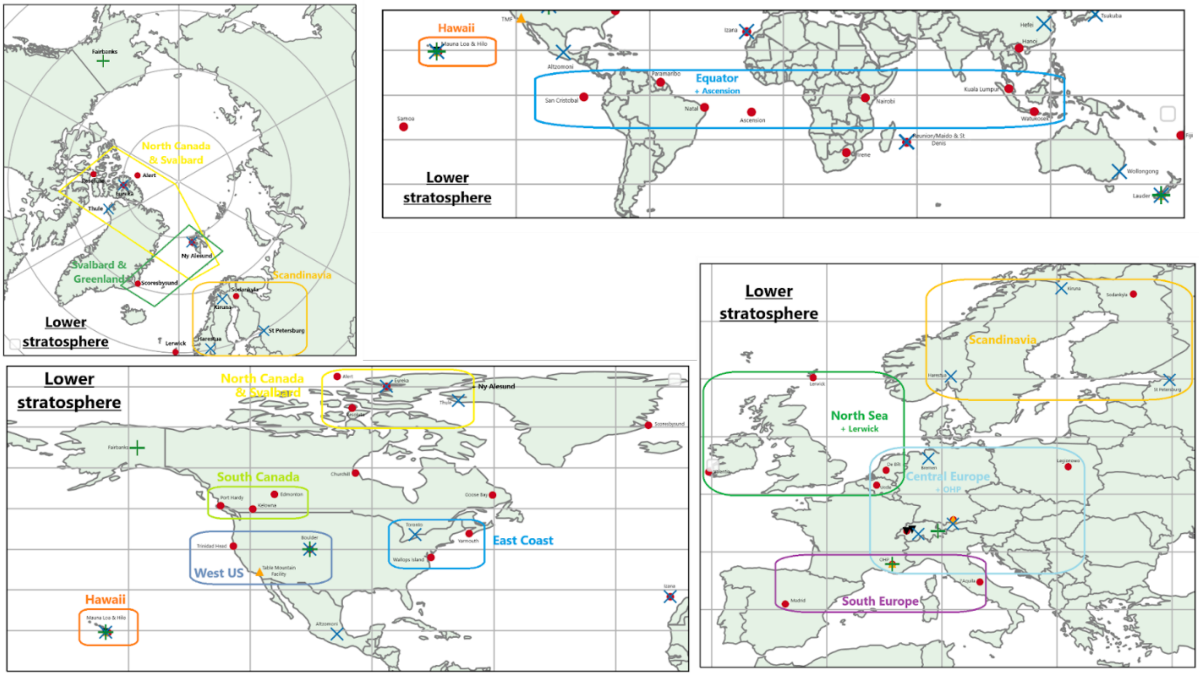

Figure S7: Maps with the groups in LS and UTLS

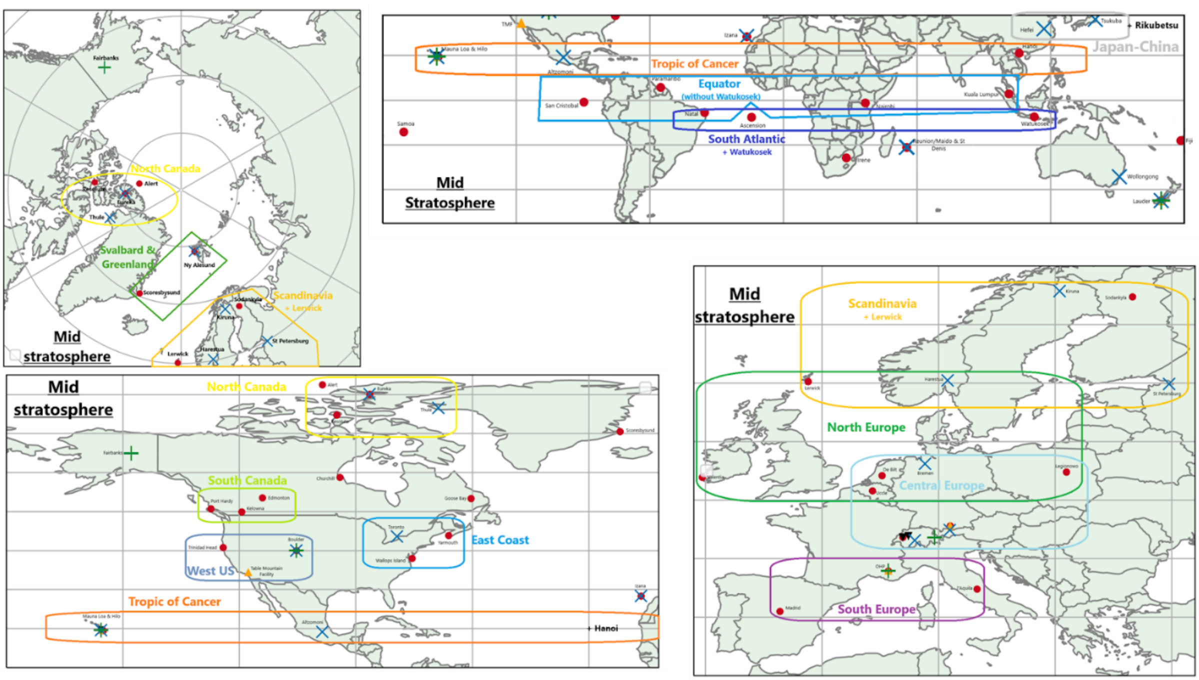

Figure S8: Maps with the groups in MS and aMS

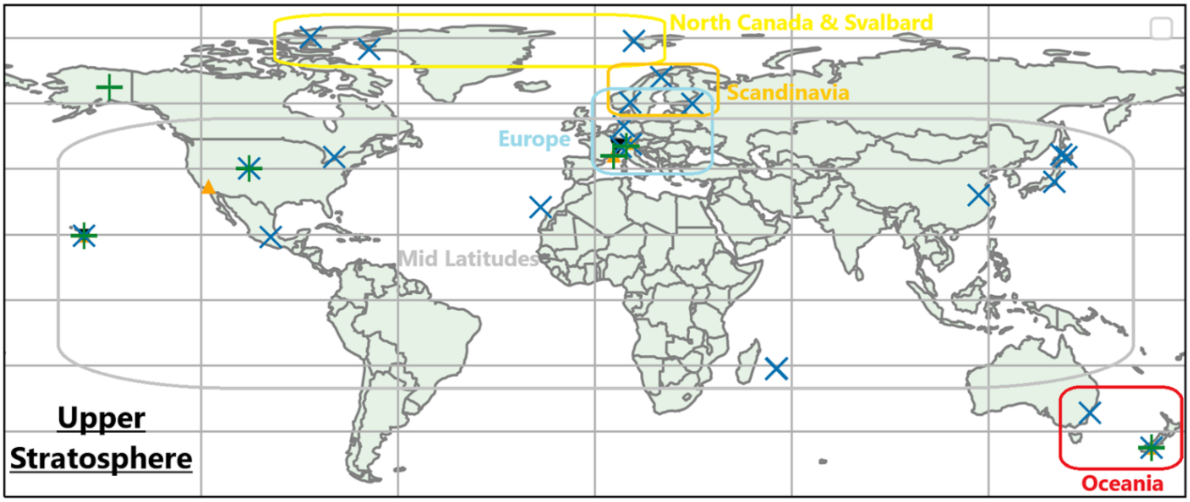

Figure S9: Map with the groups in UpS and aUpS

S7: HMC diagnostics

The Hamiltonian Monte Carlo (HMC) sampling convergence was evaluated across all regional groups and atmospheric layers using the rank-normalized Gelman-Rubin diagnostic ($\hat{R}$) and the Effective Sample Size (ESS). Overall, the algorithm demonstrates excellent stability. When evaluating the worst-case performance (maximum $\hat{R}$ and minimum ESS) across the entirety of each time series (group/layer combinations):

- For 47% of the time series, every single month achieved the strict $\hat{R} < 1.01$ threshold. Furthermore, 76% of the time series never exceeded an $\hat{R}$ of 1.05 at any month during the 2000–2024 period.
- For the ESS, 57% of the time series maintained a minimum ESS (bulk) > 400 across all months, and 62.5% maintained a minimum ESS (tail) > 400 across all months.

The months that fail to meet these thresholds mainly occur in the lower atmospheric layers (LS, UTLS, and TROPO) or for groups like north Canada. As discussed in the main text (see the August 2012 bimodal case study), these failurs correspond to inter-instrument disagreement. With a multimodal posterior probability landscape, HMC parallel chains can remain localized in separate probability maxima, leading to elevated $\hat{R}$ and reduced ESS values.